

# Leptogenesis, neutrino masses and gauge unification

N. Cosme\*,

*Service de Physique Théorique, CP225  
Université Libre de Bruxelles,  
Bld du Triomphe, 1050 Brussels, Belgium.*

## Abstract

Leptogenesis is considered in its natural context where Majorana neutrinos fit in a gauge unification scheme and therefore couple to some extra gauge bosons. The masses of some of these gauge bosons are expected to be similar to those of the heavy Majorana particles, and this can have important consequences for leptogenesis. In fact, the effect can go both ways. Stricter bounds are obtained on one hand due to the dilution of the CP-violating effect by new decay and scattering channels, while, in a re-heating scheme, the presence of gauge couplings facilitates the re-population of the Majorana states. The latter effect allows in particular for smaller Dirac couplings.

## 1 Introduction

Thermal leptogenesis [1] takes place through CP-violating decay of heavy neutrinos in the evolution of the early universe. It eventually results in the baryon/antibaryon imbalance through partial conversion of leptons to baryons around the electroweak scale. From Sakharov's conditions [2], successful leptogenesis depends on both the amount of CP-violation and the importance of the departure from equilibrium.

In the simple model, i.e. the Standard Model (SM) together with three singlet heavy Majorana neutrinos, the description of these phenomena can be accurately described by few parameters: light neutrino masses<sup>1</sup> and the lightest Majorana mass [3], [4], [5] (assuming an important hierarchy between Majorana states).

The inclusion of right-handed Majorana neutrinos is however quite difficult to justify outside some Grand Unification context (the most obvious candidate being  $SO(10)$ ). Obviously, the unification is accompanied by gauge bosons coupled to Majorana neutrinos. Irrespective of the detailed breaking scheme, we can expect that the masses of some gauge bosons will be linked to the breaking mechanism associated to the Majorana mass. As a consequence, a full description of leptogenesis should at the very least consider the part of the gauge sector linked to right-handed neutrinos, that is particles as  $W_R^\pm$  and a  $Z'$ .

While we insist that the actual breaking scheme does not need to include an explicit passage through the stage  $SU(2)_R \times U(1)$ , it is logical to include at least the above-mentioned particles in the analysis.

The inclusion of such particles can have non negligible impact on the analysis. The most straightforward is probably an extra dilution of the generated CP violation [6], and hence ultimately baryon number due to new decay and scattering channels. This will be shown in some detail below. On the other hand, the new gauge couplings will also be seen to enhance leptogenesis in some part of the parameter space, namely when the Yukawa couplings (Dirac masses) are small. In this case indeed, the presence of the larger gauge interactions favor the production of the heavy Majorana particles in a re-heating context.

As a result of both effects, we will thus find that the parameter area is both shrunk on one side, and extended to low Yukawa coupling values.

To be definite, and despite the above remark that the present considerations apply very generally in unified theories, whether the LR-symmetric stage is actually realized or not as an intermediary step of the symmetry breaking, we will use the simplest consistent structure, namely  $SU(2)_L \times SU(2)_R \times U(1)_{B-L}$  (note that the coupling constants of the two  $SU(2)$  groups need not be equal, but this translates only below in a re-definition of the gauge mass scale).

Also for definiteness, we assume that the  $SU(2)_R \times U(1)_{B-L}$  is broken by a scalar triplet of  $SU(2)_R$ ; we have also assumed that the mass of the surviving scalars are heavy enough for their effect to be neglected here (this scheme is opposite to the one considered in [7]). This scalar VEV as usual provides masses to  $W_R^\pm$  and  $Z'$  gauge bosons and a Majorana mass for right-handed neutrinos  $N$ . The high Majorana mass leads to the "see-saw" mechanism [8] for the left-handed neutrino mass through the Yukawa couplings:

$$\bar{l}_L \phi \lambda_l e_R + \bar{l}_L \tilde{\phi} \lambda_\nu N + \frac{1}{2} \bar{N}^c M N + h.c., \quad (1)$$

\*ncosme@ulb.ac.be

<sup>1</sup>that is more precisely, the quantity  $\tilde{m}_1 = (\lambda_\nu \lambda_\nu^\dagger)_{11} v^2 / M_1$  for  $\lambda_\nu$  the left-handed neutrino Yukawa couplings matrix and  $M_1$  the lightest Majorana mass.

where  $\phi$  is the SM scalar doublet, and  $l_L = \begin{pmatrix} \nu_L & e_L \end{pmatrix}^T$ .

As, announced, the expected effects include:

1. The gauge dilution of the CP-asymmetry due to a CP-invariant decay rate through the gauge sector [6], this will be dealt with in section 2.
2. A lower Majorana decoupling due to new diffusion reactions beside the one usually considered in the minimal case cf. Fig 1, 2. These additional diffusions keep heavy neutrinos at equilibrium in a wider parameter space, namely for small Majorana masses as seen below in section 4.
3. In a re-heating scenario, the probability to produce the heavy neutrino can be considerably enhanced by their gauge coupling with respect to the minimal case. This point is also discussed in section 4.

## 2 CP-Asymmetry

The lepton asymmetry originates from the leptonic number violating and CP violating decay of Majorana neutrinos ( $N_1 \rightarrow l_L \phi + N_1 \rightarrow \bar{l}_L \phi^\dagger$ ). The CP asymmetry in the decay is generated at the one loop level thanks to the complex nature of the neutrino mass matrix. In the minimal model of leptogenesis, this CP asymmetry for the lightest Majorana can be written as:

$$\varepsilon_1 = \frac{\Gamma(N_1 \rightarrow l \phi) - \Gamma(N_1 \rightarrow \bar{l} \phi^\dagger)}{\Gamma(N_1 \rightarrow l \phi) + \Gamma(N_1 \rightarrow \bar{l} \phi^\dagger)} = -\frac{3}{16\pi} \frac{1}{\left(\lambda_\nu \lambda_\nu^\dagger\right)_{11}} \sum_{i=2,3} \frac{M_1}{M_i} \text{Im} \left[ \left(\lambda_\nu \lambda_\nu^\dagger\right)_{1i}^2 \right], \quad (2)$$

in the basis of diagonal Majorana mass matrix, with  $M_1 \ll M_2 \ll M_3$ .

Even though  $\varepsilon_1$  depends on the flavor structure of the Yukawa couplings, and hence of the different unknown mass parameters, the Davidson-Ibarra bound [9] gives:

$$|\varepsilon_1| < \frac{3}{16\pi} \frac{M_1}{v^2} (m_3 - m_1). \quad (3)$$

Moreover, an improvement has been recently proposed in [10], assuming the neutrino oscillation parameters  $\Delta m_{solar}^2 \ll \Delta m_{atm}^2$ , that is:

$$|\varepsilon_1| < \frac{3}{16\pi} \frac{M_1}{v^2} (m_3 - m_1) \frac{1}{2} \sqrt{1 - \left[ \frac{(1-a)\tilde{m}_1}{(m_3 - m_1)} \right]^2} \sqrt{(1+a)^2 - \left[ \frac{(m_3 + m_1)}{\tilde{m}_1} \right]^2}, \quad (4)$$

with  $a = 2\mathcal{R}e \left[ \frac{m_1 m_3}{\tilde{m}_1^2} \right]^{1/3} \left[ -1 - i \sqrt{\frac{(m_1^2 + m_3^2 + \tilde{m}_1^2)^3}{27m_1^2 m_3^2 \tilde{m}_1^2} - 1} \right]^{1/3}$ .

This bound provides an upper estimate of the CP asymmetry based on experimental constraints, and irrespective of the specific mass pattern assumed in solar and atmospheric neutrino oscillations.

Let us turn to the decay channels for the Majorana neutrinos mediated by the extended gauge structure. Using the familiar notation  $N_1$  for the lightest Majorana state, of mass  $M_1$ , two cases can be distinguished. When  $M_1 > M_{W_R}$ , i.e. when the  $W_R$  is lighter than all Majorana particles, the additional channels will mostly occur in a two body decay into an on-shell  $W_R$ , and will be found to dilute excessively the induced CP asymmetry. For  $M_1 < M_{W_R}$  instead, the three-body decay channels will dominate.

These mostly CP conserving channels will result in a diluted CP asymmetry with respect to the minimal model, which we parametrise by  $X$ :

$$\varepsilon_1^{tot} = \frac{\varepsilon_1}{1+X}, \quad (5)$$

where the total decay width of the Majorana neutrino is  $\Gamma_{N_1}^{tot} = [\Gamma(N_1 \rightarrow l \phi) + \Gamma(N_1 \rightarrow \bar{l} \phi^\dagger)] (1+X)$ , with  $\Gamma(N_1 \rightarrow l \phi) + \Gamma(N_1 \rightarrow \bar{l} \phi^\dagger) = \left[ \left(\lambda_\nu \lambda_\nu^\dagger\right)_{11} / 8\pi \right] M_1$ .

In the first case,  $M_1 > M_{W_R}$ , the two body decay width is:

$$\Gamma_1^{2b} = \frac{g^2}{32\pi} \frac{M_1^3}{M_{W_R}^2} \left( 1 - \frac{M_{W_R}^2}{M_1^2} \right)^2 \left( 1 + 2 \frac{M_{W_R}^2}{M_1^2} \right), \quad (6)$$

which therefore implies the following dilution factor (with  $a_w = M_{W_R}^2/M_1^2$  the additional parameter which describes leptogenesis in the present case):

$$X = \frac{g^2 v^2}{4\tilde{m}_1 M_1} \frac{(1-a_w)^2 (1+2a_w)}{a_w}. \quad (7)$$

As an estimate, taking for instance  $\tilde{m}_1 \sim \mathcal{O}(10^{-4})$  eV and  $M_1 \sim \mathcal{O}(10^{11})$  GeV, which in the analysis of the minimal leptogenesis model seems to be in the allowed favored range of parameters to get a baryonic asymmetry of the order of  $n_B/s \sim \mathcal{O}(10^{-10})$ ; for  $a_w = 1/2$ , we get a dilution factor  $X \sim \mathcal{O}(10^4 - 10^5)$ . Since the dilution increases for lower  $a_w$ , the dilution due to the two-body decay channel ruins completely the produced asymmetry and leads to a non acceptable leptogenesis scheme. We will not consider here the case where the gauge boson is nearly degenerate with the Majorana particle.

For the second case,  $M_{W_R} > M_1$ , the decay width of the Majorana neutrino  $N_1$  in three bodies can be written as:

$$\Gamma_1^{3b} = \frac{3g^4}{2^{10}\pi^3} \frac{M_1^5}{M_{W_R}^4}. \quad (8)$$

The corresponding dilution factor,

$$X = \frac{3g^4 v^2}{2^7 \pi^2} \frac{1}{\tilde{m}_1 M_1 a_w^2}, \quad (9)$$

decreases rapidly with the hierarchy and for  $\tilde{m}_1 \sim \mathcal{O}(10^{-4})$  eV and  $M_1 \sim \mathcal{O}(10^{11})$  GeV with  $a_w \sim 10$  we only get a dilution  $\sim \mathcal{O}(10)$ .

We keep here the possibility of a successful leptogenesis and will therefore study the dynamical evolution in this case to reveal the characteristic features of this realistic frame, namely additional constraints, but also new windows for the re-heating scenario.

### 3 Boltzmann equations with a minimal right-handed gauge sector

In this section, we consider the extension of the standard Boltzmann equations for leptogenesis to the minimal right-handed gauge sector presented in the introduction. In this model, the Majorana mass has the same origin than the breaking of the left-right structure through the expectation value of a scalar triplet of  $SU(2)_R$ . As a consequence, interactions mediated by the gauge sector of right-handed fermions may be relevant with respect to the decoupling of Majorana neutrinos when decaying [11]. The influence of those processes on the leptogenesis efficiency depends on the relative hierarchy between the  $SU(2)_R$  gauge boson masses and the Majorana mass.

We assume here that the remaining components of the triplet scalar are heavy enough to be neglected in the evolution equations, and recall briefly the usual interactions of the scalar doublets in relation to the  $(\tilde{m}_1, M_1)$  parameters.

The decay through the scalar vertex ( $N_1 \rightarrow l_L \phi$ ) and  $\Delta L = 1$  diffusions mediated by the scalar doublet  $\phi$  (Fig. 1) are important in the Boltzmann equations with high  $\tilde{m}_1$ . Indeed, we can easily see that (see appendix A for notations of the reduced quantities appearing in the Boltzmann equations):

$$\frac{1}{H(M_1)_S} (\gamma_{D,\phi}, \gamma_{\phi,s}, \gamma_{\phi,t}) \propto \tilde{m}_1, \quad (10)$$

for  $\gamma_{D,\phi} = \gamma[(N_1 \rightarrow l_L \phi) + (N_1 \rightarrow \bar{l}_L \phi^\dagger)]$ ,  $\gamma_{\phi,s} = \gamma[(N_1 l_L \rightarrow \bar{l}_R Q)]$  and  $\gamma_{\phi,t} = \gamma[(N_1 t_R \rightarrow \bar{l}_L \bar{Q})]$ , the corresponding reaction densities. They limit therefore the Majorana decoupling for growing Yukawa couplings and imply a reduction of the leptogenesis efficiency.

For  $\Delta L = 2$  diffusions (Fig. 2), if we restrict ourselves to one Majorana neutrino in the propagator, we get:

$$\frac{\gamma_{N(t)}}{H(M_1)_S} \propto \tilde{m}_1^2 M_1, \quad (11)$$

for  $\gamma_N = \gamma[(l_L \phi \rightarrow \bar{l}_L \phi^\dagger)]$  and  $\gamma_{N,t} = \gamma[(l_L l_L \rightarrow \phi \phi^\dagger)]$ . Even though  $\gamma_N$  and  $\gamma_{N,t}$  increase with  $M_1$  in this case, the mediation through heavier Majorana neutrinos  $N_2$  and  $N_3$  strengthens this behavior. The exact evaluation of this effect is actually impossible since it depends on the  $N_2$  and  $N_3$  masses together with their Yukawa couplings to light neutrinos. We adopt therefore the parametrisation of [3, 5, 10] to take this effect into account.

Incidentally, since our goal is mainly to highlight the possible influence of interactions mediated by the  $SU(2)_R$  gauge sector, we neglect here scatterings with light SM gauge bosons as well as thermal effects and couplings renormalization which according to [5] give only  $\mathcal{O}(1)$  corrections and less.

We turn now to the discussion of  $SU(2)_R$  gauge bosons interactions. As already mentioned, since the case  $M_1 > M_{W_R}$  is completely ruined by the gauge dilution of the CP asymmetry, we only consider here interactions for  $M_1 < M_{W_R}$ . As a consequence, the dominant interactions to be added here, are the  $W_R$  and  $Z'$  - mediated scatterings. The Boltzmann equations are therefore modified by the inclusion of the following terms:

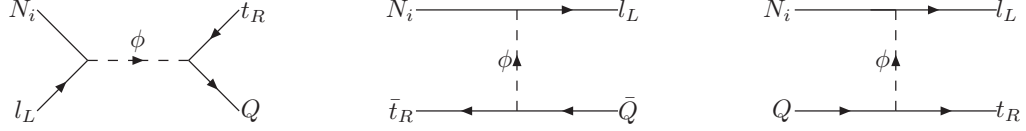


Figure 1:  $\Delta L = 1$  diffusion interactions.

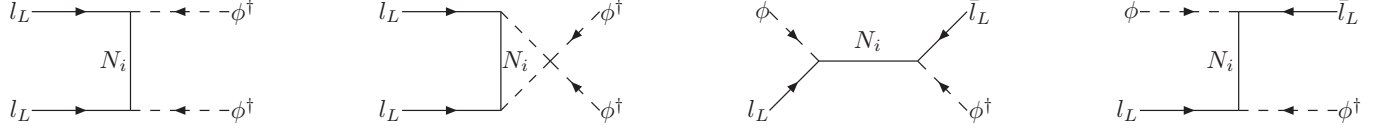


Figure 2:  $\Delta L = 2$  diffusion interactions.

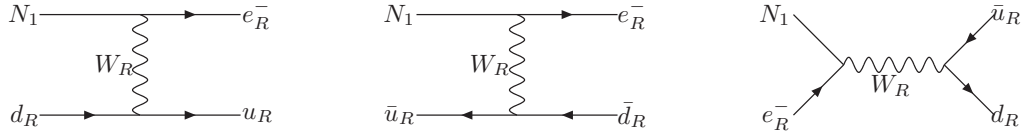


Figure 3: diffusion interaction with one  $N_1$  to be added in a gauge theory.

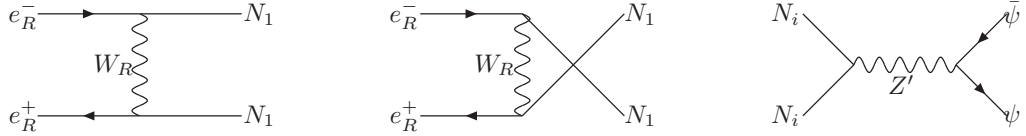


Figure 4: diffusion interaction with two  $N_1$  to be added in a gauge theory.

- the 3-body decay channels  $\gamma_{\mathcal{D}, W_R}$ , with the partial width given by (8). Note that the out of equilibrium condition  $\Gamma^{3b} < 3H$ , yields the constraint :

$$M_1 > \frac{10^{12} \text{ GeV}}{a_w^2}. \quad (12)$$

- the  $\gamma_{N_1, e_R} = \gamma[(N_1 e_R \rightarrow \bar{u}_R d_R)]$ ,  $\gamma_{N_1, u_R} = \gamma[(N_1 u_R \rightarrow \bar{e}_R d_R)]$  and  $\gamma_{N_1, d_R} = \gamma[(N_1 d_R \rightarrow e_R u_R)]$  reaction densities for all quarks families and colors, which are added in the  $Y_{N_1}(z)$  evolution equation to the standard  $\Delta L = 1$  diffusions (Figure 3).
- the  $\gamma_{N_1, N_1} = \gamma[(N_1 N_1 \rightarrow e_R \bar{e}_R, \psi \bar{\psi})]$  reaction density ( for all  $\psi$  fermions in the SM) introducing a quadratic term in  $Y_{N_1}$  (Figure 4). This reaction however suffers of one more parameter, i.e. the  $Z'$  mass. We could deal with that problem by considering the two limit cases  $M_{Z'} = M_{W_R}$  and  $M_{Z'} \rightarrow \infty$  (shown in Fig. 5). The final leptonic asymmetry would then be in between these two cases. Nevertheless numerical computation shows only irrelevant differences between these cases in the final leptogenesis efficiency. We therefore present the only case  $M_{Z'} = M_{W_R}$ . One should observe moreover that scattering mediated by the  $Z'$  boson can be neglected at energies far above the resonance. Actually, the  $W_R$ -mediated process being in the  $t$  and  $u$  channels, its reduced cross-section ( $\hat{\sigma} \sim s\sigma$ ) logarithmically grows with the center of mass energy while the  $Z'$ -mediated interaction, in the  $s$  channel, has a constant reduced cross section after the resonance.

On the other hand, even though  $Z'$  mediated processes have already been considered in [12], the inclusion here of charged current interactions has a larger impact on the evolution of Majorana neutrinos since their corresponding rates are leading and less suppressed for decreasing temperature.

All these processes are independent of the Yukawa couplings but are more efficient for lower  $M_1$ :

$$\frac{1}{H(M_1)_S} (\gamma_{\mathcal{D}, W_R}, \gamma_{N_1, e_R}, \gamma_{N_1, u_R}, \gamma_{N_1, d_R}, \gamma_{N_1, N_1}) \propto \frac{1}{M_1}. \quad (13)$$

They do not influence the wash-out of the leptonic number and mostly act in preventing the departure from equilibrium of Majorana neutrinos.

We expect a decrease of the efficiency of leptogenesis at low  $M_1$  due to these effects, depending on the ratio  $a_w$ , as can be expected from (12) and (13).

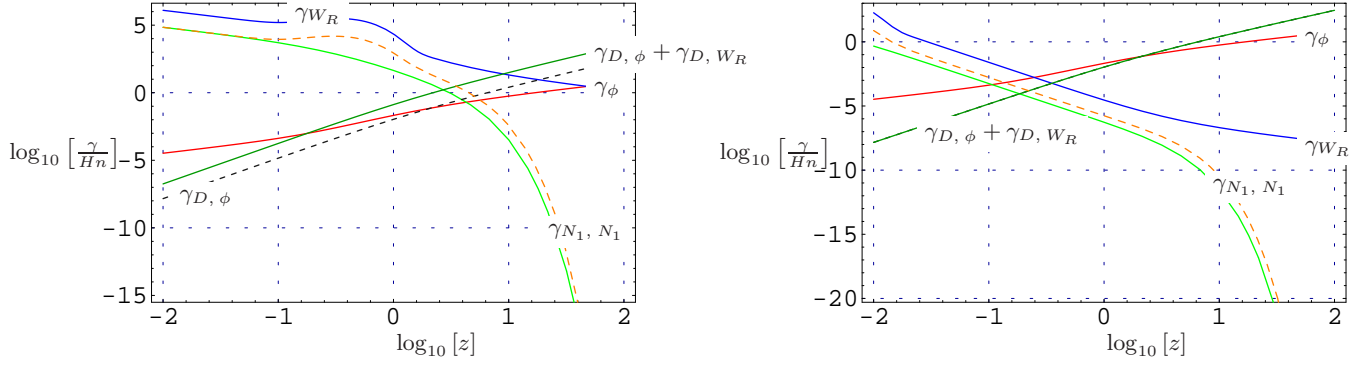


Figure 5: Examples of the competition between interactions rates in the minimal case and the gauge extended case. *Left* :  $a_w = 10^2$ ; *Right* :  $a_w = 10^6$ , both with  $\tilde{m}_1 = 10^{-5} \text{ eV}$  and  $M_1 = 10^{10} \text{ GeV}$ . The quantity  $\gamma_\phi$  (resp.  $\gamma_{W_R}$ ) is the linear coefficient involved in the Boltzmann equation for the scatterings with an intermediate  $\phi$  (resp.  $W_R$ ), i.e.  $\gamma_\phi = 2\gamma_{\phi,s} + 4\gamma_{\phi,t}$  (resp.  $\gamma_{W_R} = 2\gamma_{N_1,e_R} + 2\gamma_{N_1,d_R} + 2\gamma_{N_1,u_R}$ ). The  $N_1 - N_1$  scattering mediated by the  $SU(2)_R$  gauge bosons is also shown; the continuous line takes into account the  $W_R$  alone while the dashed line includes also the  $Z'$ .

Finally, we write the Boltzmann equations under discussion which have to be solved numerically.<sup>2</sup> Results are presented in the next section.

$$\frac{sH(M_1)}{z} \frac{dY_{N_1}}{dz} = -[\gamma_{D,\phi} + \gamma_{D,W_R} + 2\gamma_{\phi,s} + 4\gamma_{\phi,t} + 2\gamma_{N_1,e_R} + 2\gamma_{N_1,d_R} + 2\gamma_{N_1,u_R}] \left( \frac{Y_{N_1}}{Y_{N_1}^{eq}} - 1 \right) - \gamma_{N_1,N_1} \left[ \left( \frac{Y_{N_1}}{Y_{N_1}^{eq}} \right)^2 - 1 \right] \quad (14)$$

$$\frac{sH(M_1)}{z} \frac{dY_L}{dz} = -\varepsilon_1 \gamma_{D,\phi} \left[ \frac{Y_{N_1}}{Y_{N_1}^{eq}} - 1 \right] - \frac{Y_L}{Y_L^{eq}} \left[ \frac{\gamma_{D,\phi}}{2} + 2\gamma_{N,t} + 2\gamma_{\phi,t} + \frac{Y_{N_1}}{Y_{N_1}^{eq}} \gamma_{\phi,s} \right] \quad (15)$$

## 4 Matter asymmetry and leptogenesis efficiency

The present baryonic asymmetry of the universe is quantified by the ratio between the net number of baryons and the number of photons in the universe. From nucleosynthesis analysis and measurements on the cosmic microwave background, one can deduce the very smallness of this asymmetry, i.e. according to the recent WMAP results [13]:

$$\frac{n_B}{n_\gamma} = (6.1^{+0.3}_{-0.2}) 10^{-10}. \quad (16)$$

In order to explain this quantity through the leptogenesis process, once a lepton asymmetry is produced, we require the conversion of this non-zero lepton number in a non-zero baryon number [14]. This conversion is provided by non-perturbative electroweak interactions, as exemplified by sphalerons which take place around the electroweak phase transition and conserve  $B - L$  while violating both  $B$  and  $L$ . A complete conversion would lead to  $B_{final} = -1/2 L_{initial}$  but is usually evaluated to  $B_{final} = -28/79 L_{initial}$  [15].

Now, in the most favorable case, the maximal lepton asymmetry produced by the Majorana neutrino decay can be estimated as  $Y_L^{final} = \varepsilon_1 Y_{N_1}^{eq}(init.)$ , where  $Y_{N_1}^{eq}(init.)$  is the initial equilibrium  $N_1$  abundance. However, the leptogenesis efficiency is not always maximal and depends mainly on the importance of the departure from equilibrium and the possible wash-out of the produced lepton asymmetry by  $\Delta L \neq 0$  diffusions. We can easily write an analytical expression for the efficiency using the integral form of the Boltzmann equation for the lepton number:

$$\eta_{eff} = \int_0^\infty dt \frac{z(Y_{N_1} - Y_{N_1}^{eq})}{sH(M_1)Y_{N_1}^{eq}(init.)^2} \gamma_{D,\phi} \text{Exp} \left[ - \int_t^\infty dx W_L(x) \right], \quad (17)$$

<sup>2</sup>We do not consider here an evolution equation for the leptonic number of right-handed fermions since we assume no CP asymmetry in that sector, which is treated here at tree level.

for  $W_L(z) = \frac{z}{sH(M_1)Y_{N_1}^{eq}} \left( \frac{\gamma_{D,\phi}}{2} + 2\gamma_N + 2\gamma_{N,t} + 2\gamma_{\phi,t} + \frac{Y_{N_1}}{Y_{N_1}^{eq}} \gamma_{\phi,s} \right)$  the wash-out terms of the leptonic asymmetry. The efficiency does not depend on the CP asymmetry and characterizes therefore the intrinsic dynamics of the leptogenesis process in a given theory.

As a consequence, depending on the parameters, we can express the final leptonic asymmetry including the efficiency by:

$$\frac{n_L^{final}}{s} = Y_L^{final} = \varepsilon_1 Y_{N_1}^{eq}(init.) \eta_{eff}. \quad (18)$$

Finally, the baryons to photons ratio is evaluated in term of leptogenesis quantities to :

$$\frac{n_B}{n_\gamma} \simeq 7 \frac{28}{79} Y_{B-L} = -\frac{196}{79} \varepsilon_1 Y_{N_1}^{eq}(init.) \eta_{eff}, \quad (19)$$

where the factor 7 holds for  $s/n_\gamma$ .

We present results for the leptogenesis efficiency  $\eta_{eff}$  as a function of  $\tilde{m}_1$ ,  $M_1$  and  $a_w$  the  $W_R$  to Majorana mass squared ratio in Figure 6.

Both thermal and zero initial Majorana abundance scenarios are shown but, however, with respect to the minimal leptogenesis scheme which is significantly more constrained by a zero initial Majorana abundance, the extended gauge model shows less dependency according to these cases even for a sizable hierarchy. Indeed, as one can easily expect, the creation of heavy Majorana neutrinos is not anymore a problem once they are allowed to take part in gauge interactions. This effect remains up to ratios of the order  $a_w \propto 10^6$  in the relevant  $M_1$  range.

The second interesting consequence of the inclusion of  $W_R$  mediated diffusions is a drastic reduction of leptogenesis efficiency for low Majorana masses which increases dramatically for low  $a_w$ -ratio. This comes from both delayed (or impeded) decoupling of Majorana neutrinos through additional diffusions and decay channels: the final leptonic asymmetry is therefore reduced.

Now, in order to discuss the baryon number, we have to link observables on neutrino oscillations and the CP asymmetry in the decay of the lightest Majorana (4). As already proposed by [5] and for the purpose of comparison, we consider the sample case where  $m_3 = \max(\tilde{m}_1, \sqrt{\Delta m_{atm}^2})$  with  $m_3^2 - m_1^2 = \Delta m_{atm}^2$ . Combining equations (4) and (19) therefore provides an upper estimate of the baryons to photons ratio.

Figure 7 shows the iso- $n_b/n_\gamma$  curves in the  $(\tilde{m}_1, M_1)$  plane obtained for different  $a_w$ -ratios, assuming the central value of baryon asymmetry obtained from WMAP (16). Successful leptogenesis occurs in the region bounded by the curves.

We can then extract a lower limit on the Majorana mass according to the  $W_R$  to Majorana mass squared ratio:

$a_w = M_{W_R}^2/M_1^2$	$M_1 > (\text{GeV})$
$10^4$	$\sim 10^9$
$10^2$	$\sim 10^{10}$
10	$\sim 10^{11}$
2	$\sim 10^{12}$

As already mentioned above, the case with zero initial Majorana abundance scenario (after assumed re-heating) is almost indistinguishable in our framework from the case of a thermal initial abundance. Consequently, in the case of re-heating, we allow, despite the dilution, for broader windows in some domains of the parameters.

For comparison, the minimal (non-gauged Majorana) model curve for an initial thermal Majorana abundance coincides in practice with our curve for  $a_w = 10^6$  (the latter, irrespective of the thermal or re-heating scenario).

## 5 Conclusion

Inspired by a grand-unified framework necessary to understand the presence of heavy Majorana particles, we considered the addition of a minimal gauge sector for right-handed neutrinos and derived its consequences on baryon number in both the thermal decay and re-heating scenarios.

The results are :

- a diluted CP asymmetry due to new Majorana decay channels through gauge bosons, restricting successful leptogenesis to the case  $M_{W_R} > M_1$  [6];
- a reduction of the leptogenesis efficiency for low  $W_R$  to Majorana mass squared ratio ( for  $a_w < 10^4$ );
- in the re-heating scenario, an enhanced production of Majorana neutrinos thanks to their gauge interactions ( up to  $a_w \sim 10^6$ ).



The consequences from the baryon to photon ratio on the neutrino mass parameters with respect to the minimal scheme is a higher Majorana mass for decreasing  $W_R$  to Majorana mass ratio and a broader window in the case of zero initial Majorana abundance (see Figure 7).

## Acknowledgments

I would like to thank especially J.-M. Frère for his advice and support all along this work. I also thank P. Aliani, M. Fairbairn, F.-S. Ling and M.H.G. Tytgat for interesting discussions. This work is supported in part by IISN, la Communauté Française de Belgique (ARC), and the belgian federal government (IUAP-V/27).

## A Boltzmann equations

We quickly summarize the conventions we used in the text with respect to the evolution equations of leptogenesis. The particle density is define as :

$$n_a = g_a \int \frac{d^3 p}{(2\pi)^3} f_a(\mathbf{p}), \quad (20)$$

where  $g_a$  is the number of internal degrees of freedom of the particle and  $f_a$  is the corresponding statistics. We assume here the Maxwell-Boltzmann statistics, so that we can re-write:

$$n_a = \frac{g_a M_a^2 T}{2\pi^2} K_2(M_a/T), \quad (21)$$

which is the equilibrium number density ( $K_n(x)$  is the modified Bessel function of order  $n$ ).

The evolution equations can then be written in term of the number of particles per comoving volume,  $Y_a(z) = n_a(z)/s(z)$  (where  $s(z)$  is the entropy density,  $z = M_1/T$ ), which is not affected by the expansion of the universe :

$$\frac{dY_a}{dz} = -\frac{z}{H(z=1)s(z)} \sum_{a,I,J} \left[ \frac{Y_a Y_I}{Y_a^{eq} Y_I^{eq}} \gamma(aI \rightarrow J) - \frac{Y_J}{Y_J^{eq}} \gamma(J \rightarrow aI) \right]. \quad (22)$$

They constitute in general a set of coupled differential equations for all particles species in the model. The  $\gamma_{(aI \rightarrow J)}$  are the reaction densities for the  $(aI \rightarrow J)$  interactions which is given for a decay process by:

$$\gamma_D = n_a^{eq} \frac{K_1(z)}{K_2(z)} \Gamma_D, \quad (23)$$

(where  $\Gamma_D$  is the usual decay width) and for a two-body scattering by ( $x = s/M_1^2$ ,  $\sqrt{s}$  the center of mass energy):

$$\gamma(aI \rightarrow J) = \frac{M_1^4}{64\pi^4 z} \int_{x_{min}}^{\infty} dx \hat{\sigma}(aI \rightarrow J)(x) \sqrt{x} K_1(z\sqrt{x}). \quad (24)$$

## B Reduced cross sections

The reduced cross sections are the kinematic ingredients from Feynman graphs that are involved in Boltzmann equations. For a given process, they can be computed through:

$$\frac{d\hat{\sigma}}{dt} = \frac{1}{8\pi s} |\mathcal{M}(aI \rightarrow J)|^2, \quad (25)$$

in terms of the Mandelstam variables ( $|\mathcal{M}(aI \rightarrow J)|^2$  being the squared amplitude summed over all internal degrees of freedom of  $a$ ,  $I$  and  $J$ ). The reduced cross section is related to the usual cross section by  $\hat{\sigma}(s) = (8/s)[(p_a \cdot p_I)^2 - m_a^2 m_I^2] \sigma(s)$ .

We list below the reduced cross section used for the relevant minimal model interactions (see e.g. [16], [12], [5], [17]):

$$x = \frac{s}{M_1^2}, \quad a_\Gamma = \frac{\Gamma_{N_1}^{D2}}{M_1^2}, \quad D_{N_1} = \frac{1}{x-1+i\sqrt{a_\Gamma}}, \quad D_{N_1}^{2,subs} = \frac{(x-1)^2 - a_\Gamma}{[(x-1)^2 + a_\Gamma]^2}, \quad (26)$$

where  $D_{N_1}^{2,subs}$  is the  $N_1$  propagator amplitude without its resonant part as suggested in [5] which avoid the double counting of real Majorana's in the inverse decay and in the  $\Delta L = 2$  diffusions.

$\Delta L = 2$  (mediated by the  $N_1$  alone):

- $l_L \phi \rightarrow \bar{l}_L \phi^\dagger$

$$\hat{\sigma}_{N_1} = \frac{1}{4\pi} (\lambda \lambda^\dagger)_{11}^2 \left[ x D_{N_1}^{2\text{subs}} + 2 \left( 1 - \frac{1}{x} \log[x+1] \right) + 4\mathcal{R}e[D_{N_1}] \left( 1 - \frac{x-1}{x} \log[x+1] \right) \right] \quad (27)$$

- $l_L l_L \rightarrow \phi^\dagger \phi^\dagger$

$$\hat{\sigma}_{N_1} = \frac{1}{2\pi} (\lambda \lambda^\dagger)_{11}^2 \left[ \frac{x}{(x+1)} + \frac{2}{2+x} \log[x+1] \right] \quad (28)$$

$\Delta L = 1$ :

- $N_1 l_L \rightarrow \bar{l}_R Q$

$$\hat{\sigma} = \frac{3}{4\pi} (\lambda \lambda^\dagger)_{11} \frac{m_t^2}{v^2} \left( \frac{x-1}{x} \right)^2 \quad (29)$$

- $N_1 t_R \rightarrow \bar{l}_L Q$

$$\hat{\sigma} = \frac{3}{4\pi} (\lambda \lambda^\dagger)_{11} \frac{m_t^2}{v^2} \left( \frac{x-1}{x} + \frac{1}{x} \log \left[ \frac{x-1+a_\phi}{a_\phi} \right] \right), \quad (30)$$

where  $a_\phi = m_\phi^2/M_1^2$  is an infra-red regulator chosen such that  $m_\phi \sim 800\text{GeV}$  [12].

Since we include extra gauge bosons in the model, we list below the reduced cross-sections for the relevant  $SU(2)_R$  diffusions:

$$a_{w(Z')} = \frac{M_{W_R(Z')}^2}{M_1^2} \quad a_{\Gamma_{W_R(Z')}} = \frac{\Gamma_{W_R(Z')}^2}{M_1^2}. \quad (31)$$

- $N_1 d_R \rightarrow e_R u_R$

$$\hat{\sigma} = \frac{9g^4}{8\pi a_w} \frac{(x-1)^2}{(x+a_w-1)}, \quad (32)$$

- $N_1 u_R \rightarrow \bar{e}_R d_R$

$$\hat{\sigma} = \frac{9g^4}{8\pi x} \int_{(1-x)}^0 dt \frac{(x+t-1)(x+t)}{(t-a_w)^2}, \quad (33)$$

- $N_1 e_R \rightarrow \bar{u}_R d_R$

$$\hat{\sigma} = \frac{9g^4}{8\pi x [(x-a_w)^2 + a_w a_{\Gamma_{W_R}}]} \int_{(1-x)}^0 dt (x+t)(x+t-1), \quad (34)$$

- $N_1 N_1 \rightarrow e_R \bar{e}_R, \psi \bar{\psi}$

$$\hat{\sigma}_{W_R} = \frac{g^4}{8\pi x} \int_{t_0}^{t_1} dt \left[ \frac{(x+t-1)^2}{[t-a_w]^2} + \frac{(1-t)^2}{[2-a_w-x-t]^2} - \frac{2x}{[t-a_w][2-a_w-x-t]} \right], \quad (35)$$

$$\hat{\sigma}_{Z'} = \frac{g^4 R_{N_1}^2}{3 \cdot 2^5 \pi c_w^4} \frac{\sqrt{x(x-4)}(x-1)^2}{[(x-a_{Z'})^2 + a_{Z'} a_{\Gamma_{Z'}}]} [9R_{u_R}^2 + 9R_{d_R}^2 + 3R_{e_R}^2 + 6L_{e_L}^2 + 18L_{q_L}^2] \quad (36)$$

$$R_f = \sqrt{c_w^2 - s_w^2} \left( 2T_R^3 - s_w^2 \frac{(B-L)}{c_w^2 - s_w^2} \right), \quad L_f = -\frac{s_w^2(B-L)}{\sqrt{c_w^2 - s_w^2}} \quad (37)$$

with  $t_0(t_1)$  the kinematic limits on the  $t$  variable. The minus sign in the interference term of  $\hat{\sigma}_{W_R}$  is due to the relative sign between the  $t$  and the  $u$  diagrams coming from Fermi-Dirac statistic. Note that for  $N_1 N_1 \rightarrow e_R \bar{e}_R$  interferences between  $s$  channel with an intermediate  $Z'$  and  $t$  and  $u$  channels mediated by a  $W_R$  cancel out for the same reason.

We also write the  $SU(2)_R$  gauge vertices added to the minimal model of leptogenesis ( with  $\Psi^{(R,L)} = ( \psi_u^{(R,L)} \quad \psi_d^{(R,L)} )^T$  ) :

$$\frac{g}{\sqrt{2}} (\bar{\psi}_u^R W_R^- \psi_d^R + h.c.), \quad (38)$$

$$g \frac{\sqrt{c_w^2 - s_w^2}}{c_w} \bar{\Psi}_R \not{Z}' \left[ T_R^3 - \frac{B-L}{2} \frac{s_w^2}{c_w^2 - s_w^2} \right] \Psi_R + \Psi_R \rightarrow \Psi_L, \quad (39)$$

where  $s_w = \sin \theta_w = -\frac{g'}{\sqrt{g^2 + 2g'^2}}$ ,  $W_R^\pm = \frac{W_R^1 \mp iW_R^2}{\sqrt{2}}$ ,  $Z' = \frac{1}{c_w} [\sqrt{c_w^2} W_R^3 + s_w B]$ ,  $g$  and  $g'$  respectively the  $SU(2)$ 's and  $U(1)$  couplings,  $W_R^a$  the  $a$ -th gauge component of  $SU(2)_R$  and  $B$  the  $U(1)$  gauge field.



## References

- [1] M. Fukugita and T. Yanagida, Phys. Lett. B **174** (1986) 45.
- [2] A. D. Sakharov, Pisma Zh. Eksp. Teor. Fiz. **5** (1967) 32 [JETP Lett. **5** (1967 SOPUA,34,392-393.1991 UFNAA,161,61-64.1991) 24].
- [3] R. Barbieri, P. Creminelli, A. Strumia and N. Tetradis, Nucl. Phys. B **575** (2000) 61 [arXiv:hep-ph/9911315].
- [4] W. Buchmuller, P. Di Bari and M. Plumacher, Nucl. Phys. B **643** (2002) 367 [arXiv:hep-ph/0205349], Nucl. Phys. B **665** (2003) 445 [arXiv:hep-ph/0302092].
- [5] G. F. Giudice, A. Notari, M. Raidal, A. Riotto and A. Strumia, Nucl. Phys. B **685** (2004) 89 [arXiv:hep-ph/0310123].
- [6] S. Carlier, J. M. Frere and F. S. Ling, Phys. Rev. D **60** (1999) 096003 [arXiv:hep-ph/9903300].
- [7] J. M. Frere, F. S. Ling, M. H. G. Tytgat and V. Van Elewyck, Phys. Rev. D **60** (1999) 016005 [arXiv:hep-ph/9901337].
- [8] T. Yanagida, KEK report 79-18 (1979), p.95. M. Gell-Mann, P. Ramond and R. Slansky, Print-80-0576 (CERN), in Supergravity, P. van Nieuwenhuizen & D.Z. Freedman (eds.), North Holland Publ. Co., 1979. Published in Stony Brook Wkshp.1979:0315 . R. N. Mohapatra and G. Senjanovic, Phys. Rev. Lett. **44** (1980) 912.
- [9] S. Davidson and A. Ibarra, Phys. Lett. B **535** (2002) 25 [arXiv:hep-ph/0202239].
- [10] T. Hambye, Y. Lin, A. Notari, M. Papucci and A. Strumia, arXiv:hep-ph/0312203.
- [11] R. N. Mohapatra and X. Zhang, Phys. Rev. D **46** (1992) 5331. E. Ma, S. Sarkar and U. Sarkar, Phys. Lett. B **458** (1999) 73 [arXiv:hep-ph/9812276]. P. Adhya, D. R. Chaudhuri and A. Raychaudhuri, Eur. Phys. J. C **19** (2001) 183 [arXiv:hep-ph/0006260].
- [12] M. Plumacher, Z. Phys. C **74** (1997) 549 [arXiv:hep-ph/9604229].
- [13] C. L. Bennett *et al.*, Astrophys. J. Suppl. **148** (2003) 1 [arXiv:astro-ph/0302207].
- [14] V. A. Kuzmin, V. A. Rubakov and M. E. Shaposhnikov, Phys. Lett. B **155** (1985) 36.
- [15] S. Y. Khlebnikov and M. E. Shaposhnikov, Nucl. Phys. B **308** (1988) 885. J. A. Harvey and M. S. Turner, Phys. Rev. D **42** (1990) 3344.
- [16] M. A. Luty, Phys. Rev. D **45** (1992) 455.
- [17] A. Pilaftsis and T. E. J. Underwood, arXiv:hep-ph/0309342.

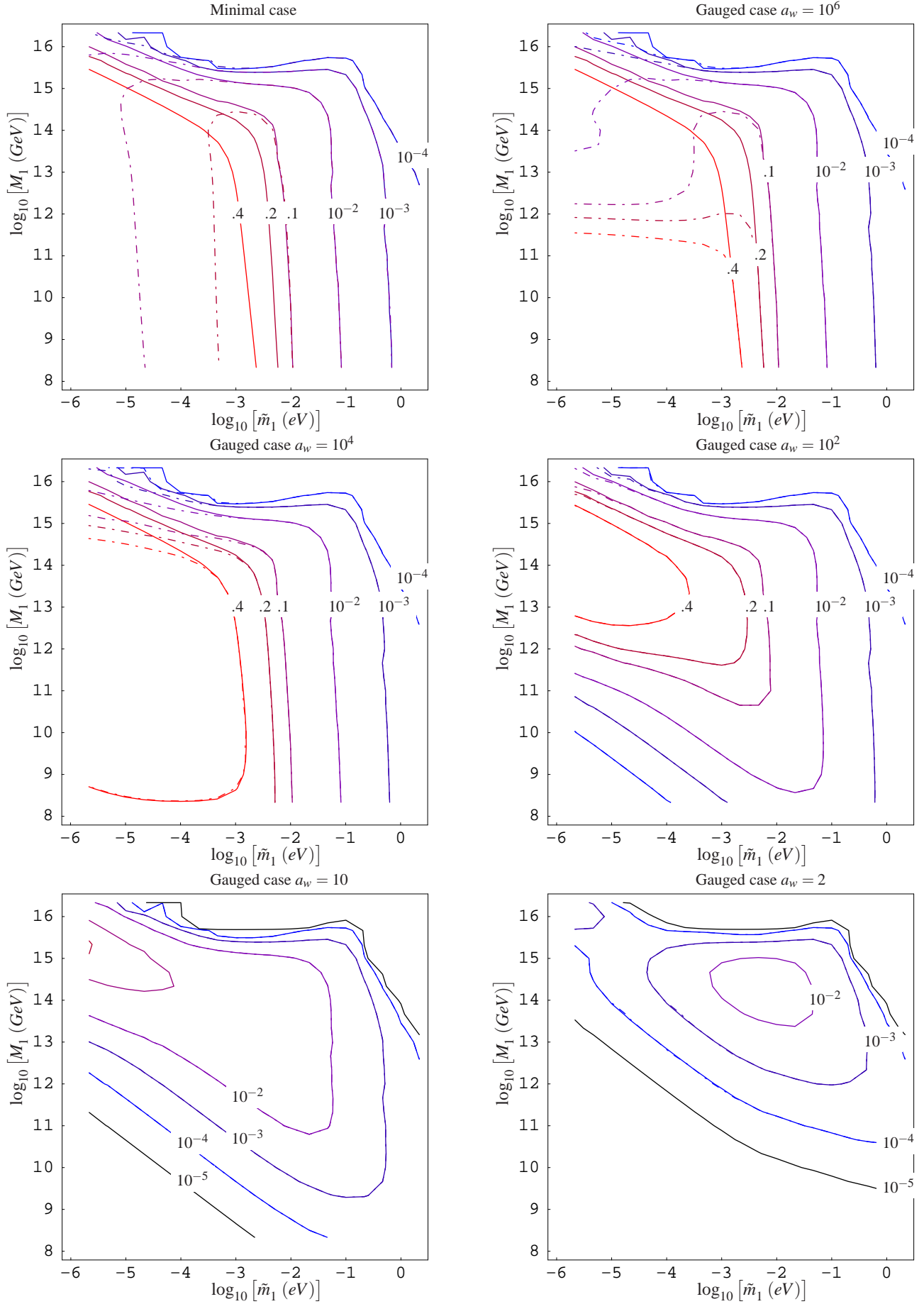


Figure 6: Efficiency of leptogenesis for the minimal case  $a_w \rightarrow \infty$  and the extended case to a minimal right-handed gauge sector for  $a_w = M_{W_R}^2/M_1^2 = 10^6, 10^4, 10^2, 10, 2$ . The continuous line is the efficiency for a thermal initial Majorana abundance while the dashed-dotted line is for a zero initial Majorana abundance.

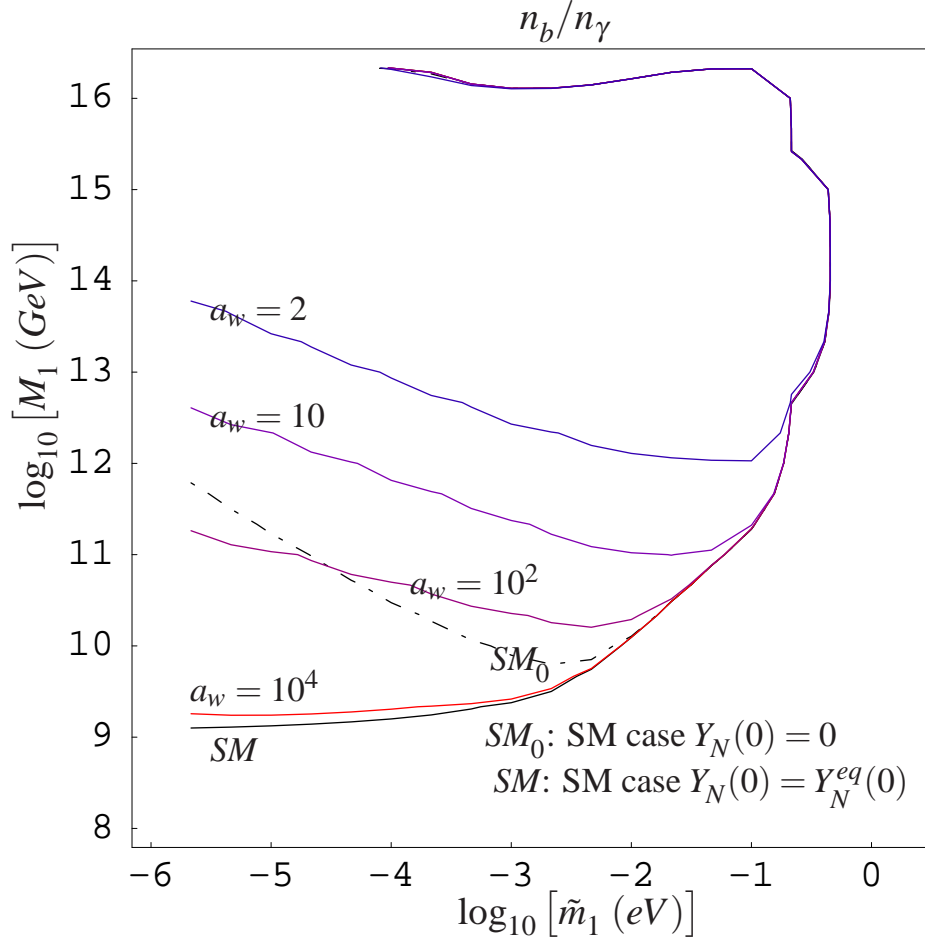


Figure 7: Limits on the baryon to photon ratio in an extended model to a minimal right-handed gauge sector with  $a_w = M_{\tilde{W}_R}^2/M_1^2 = 10^4, 10^2, 10, 2$ , from bottom to top (red to blue). The minimal SM case is also shown in black: the continuous line is for a thermal initial Majorana abundance while the dashed-dotted line is for a zero initial Majorana abundance. The matter asymmetry is higher than the WMAP value in the region bounded by the curves.